11594 *Inorg. Chem.* **2009**, *48*, 11594–11600
DOI: 10.1021/ic901462t

Inorganic Chemistry
Article

Synthesis, Characterization, and Magnetism of Divalent Aryl Transition-Metal Complexes of the Simplest Dialkylamide, NMe_2: Rare T-Shaped Coordination at Chromium

Chengbao Ni,[†] Gary J. Long,[‡] Fernande Grandjean,[§] and Philip P. Power*[,†]

[†]*Department of Chemistry, University of California, Davis, One Shields Avenue, California 95616,* [‡]*Department of Chemistry, Missouri University of Science and Technology, University of Missouri, Rolla, Missouri 65409-0010, and* [§]*Department of Physics, B5, University of Liège, B-4000 Sart-Tilman, Belgium*

Received July 23, 2009

The synthesis and characterization of a series of first-row aryl transition metal derivatives of the simplest dialkylamido ligand NMe_2 are reported. The complexes $Cr\{Ar'Cr(\mu\text{-}NMe_2)_2\}_2$ (**1**) and $\{Ar'M(\mu\text{-}NMe_2)\}_2$ (M = Mn (**2**), Fe (**3**); Ar′ = C_6H_3-2,6-(C_6H_3-2,6-$^iPr_2$)$_2$) were obtained by reaction of the aryl metal halides $\{Ar'M(\mu\text{-}X)\}_2$ (M = Cr, X = Cl; M = Fe, X = Br) or $\{Li(THF)Ar'MnI_2\}_2$ with $LiNMe_2$ in a 1:2 ratio. A similar reaction of $\{Ar^{\#}Co(\mu\text{-}I)\}_2$ ($Ar^{\#}$ = C_6H_3-2,6-(C_6H_2-2,4,6-Me_3)$_2$) and $LiNMe_2$ in hexanes gave the unusual complex $\{Ar^{\#}Co(\mu\text{-}I)(\eta^1\text{-}CH_2{=}NCH_3)\}_2$ (**4**), in which the NMe_2 ligand is dehydrogenated to afford a complexed imine. Complexes **1**−**4** were characterized by X-ray crystallography, UV−vis spectroscopy, and magnetic measurements. In the unique trinuclear complex **1**, the central chromium(II) ion is bound to four NMe_2 groups in a square planar fashion. The NMe_2 groups also bridge to the two outer chromium(II) ions, which are bound to a terminal Ar′ group to yield a rare example of three-coordinate T-shaped geometry at these atoms. In the dimers **2** and **3**, each metal center is coordinated to a terminal terphenyl ligand and two bridging NMe_2 groups to give a distorted trigonal planar geometry. In contrast, the reaction of $LiNMe_2$ with $\{Ar^{\#}Co(\mu\text{-}I)\}_2$ in a 2:1 ratio did not yield an amido product; instead, the NMe_2 ligand underwent hydrogen elimination. As a result, in the dimeric structure of **4**, each cobalt ion is coordinated to a terphenyl ligand, two bridging iodides, and a neutral methylimine ligand, $CH_2{=}NCH_3$, to yield a very distorted tetrahedral cobalt(II) coordination environment. The magnetic properties of **1**−**4** revealed antiferromagnetic exchange coupling between the metal ions with $J = -47(1)$ cm^{-1} and $J_{13} = -25(1)$ cm^{-1} for **1**, $J = -38(1)$ cm^{-1} for **2**, $J = -75(3)$ cm^{-1} for **3**, and $J = -32(4)$ cm^{-1} for **4**; the latter compound exhibited an unusually large temperature independent contribution to its molar magnetic susceptibility.

Introduction

Transition metal amides, that is, transition metal compounds incorporating an M-NR_2 moiety, where M is a transition metal ion; R is an alkyl, aryl, silyl, or related group,[1] are of current interest for numerous reasons that include their use in olefin polymerization,[2,3] C—H bond activation or hydroamination reactions,[4−7] the catalysis of C—N bond formation,[8−13] nitrogen fixation,[14−17] and metal vapor deposition.[18,19] A huge variety of amido ligands have been employed across the transition metal series including numerous types of multidentate, delocalized, and sterically crowded species. In the latter case, several bulky amido ligands have been used to isolate and characterize a number of two and three coordinate transition metal complexes.[20−26] Simpler

*To whom correspondence should be addressed. E-mail: pppower@ucdavis.edu.

(1) Lappert, M. F.; Power, P. P.; Sanger, A. R.; Srivastava, R. C. *Metal and Metalloid Amides: Syntheses, Structures, and Physical and Chemical Properties*; Ellis Horwood: Chichester, U. K., 1980, Chapter 8.
(2) McKnight, A. L.; Waymouth, R. M. *Chem. Rev.* **1998**, *98*, 2587.
(3) Gibson, V. C.; Spitzmesser, S. K. *Chem. Rev.* **2003**, *103*, 283.
(4) Bryndza, H. E.; Tam, W. *Chem. Rev.* **1988**, *88*, 1163.
(5) Roundhill, D. M. *Chem. Rev.* **1992**, *92*, 1.
(6) Holland, P. L.; Andersen, R. A.; Bergman, R. G. *Comments Inorg. Chem.* **1999**, *21*, 115.
(7) Fulton, J. R.; Holland, A. W.; Fox, D. J.; Bergman, R. G. *Acc. Chem. Res.* **2002**, *35*, 44.
(8) Odom, A. L. *Dalton Trans.* **2005**, 225.
(9) Hartwig, J. F. *Angew. Chem., Int. Ed.* **1998**, *37*, 2047.
(10) Yang, B. H.; Buchwald, S. L. *J. Organomet. Chem.* **1999**, *576*, 125.
(11) Buchwald, S. L.; Mauger, C.; Mignani, G.; Scholz, U. *Adv. Synth. Catal.* **2006**, *348*, 23.
(12) Mindiola, D. J. *Acc. Chem. Res.* **2006**, *39*, 813.
(13) Gunnoe, T. B. *Eur. J. Inorg. Chem.* **2007**, 1185.
(14) Cummins, C. C. *Chem. Commun.* **1998**, 1777.
(15) Gambarotta, S.; Scott, J. *Angew. Chem., Int. Ed.* **2004**, *43*, 5298.
(16) MacKay, B. A.; Fryzuk, M. D. *Chem. Rev.* **2004**, *104*, 385.
(17) Schrock, R. R. *Acc. Chem. Res.* **2005**, *38*, 955.
(18) Hoffman, D. M. *Polyhedron* **1994**, *13*, 1169.
(19) Just, O.; Rees, W. S. *Adv. Mater. Opt. Electron.* **2000**, *10*, 213.
(20) Bradley, D. C. *Chem. Br.* **1975**, *11*, 393.
(21) Eller, P. G.; Bradley, D. C.; Hursthouse, M. B.; Meek, D. W. *Coord. Chem. Rev.* **1977**, *24*, 1.
(22) Power, P. P. *Comments Inorg. Chem.* **1989**, *8*, 177.
(23) Power, P. P. *Chemtracts: Inorg. Chem.* **1994**, *6*, 181.
(24) Alvarez, S. *Coord. Chem. Rev.* **1999**, *193*, 13.
(25) Power, P. P. *J. Organomet. Chem.* **2004**, *689*, 3904.
(26) Cummins, C. C. *Prog. Inorg. Chem.* **1998**, *47*, 685.

Published on Web 11/13/2009

ligands, such as the parent dialkylamido ligand $-NMe_2$, have received less recent attention. Although the $-NMe_2$ ligand played a key role in the development of group 4 and 5 and saturated second and third row group 6 transition metal amides, it is seldom employed for the middle or late first-row transition metals. There are very few structurally characterized NMe_2 derivatives for the metals chromium through nickel for example. It is believed that such compounds are unstable because of associative reactions leading to decomposition.[1] For Cr−Ni, the known amido derivatives are usually derivatives of bulky ligands, such as $\{M(\mu\text{-}N^iPr_2)(N^iPr_2)\}_2$ (M = Cr or Mn),[27,28] $Mn\{N(SiMePh_2)_2\}_2$,[29] $Fe\{N(SiMe_3)_2\}_n$ (n = 2 or 3),[30,31] $Co\{N(SiMe_3)_2\}_3$,[32] or $Ni\{NPhBMes_2\}_2$,[33] in which high association numbers and decomposition are prevented by steric effects. Only a few NMe_2 derivatives have been structurally characterized for these metals, and are limited to the chromium dimer $\{(\eta^5\text{-}C_5H_5)Cr(NO)(\mu\text{-}NMe_2)\}_2$,[34] the heterometallic species $H_3C_6\text{-}1,3\text{-}\{C(CH_2)N(C_6H_3\text{-}2,6\text{-}^iPr_2)\}_2Fe(\mu\text{-}NMe_2)K(OEt_2)_2$,[35] and the hetero-bridged binuclear cobalt complex $(\eta^5\text{-}C_5Me_5)Co(\mu\text{-}Cl)(\mu\text{-}NMe_2)Co(\eta^5\text{-}C_5Me_5)$.[36] Herein, we describe the synthesis and characterization of $-NMe_2$ derivatives of Cr, Mn, and Fe stabilized by bulky terphenyl coligands.[37,38] In addition, we report an unusual reaction between $LiNMe_2$ and a cobalt aryl halide in which the $-NMe_2$ group is dehydrogenated to form an unusual imine complex.

Experimental Section

General Procedures. All manipulations were carried out by using modified Schlenk techniques under an argon atmosphere or in a Vacuum Atmospheres HE-43 dry box. All of the solvents were dried over an alumina column, stored over 3 Å molecular sieves overnight, and freeze−thaw degassed three times prior to use. The metal halide precursors were prepared according to literature procedures.[39] $LiNMe_2$ was purchased from Acros Organics and stored in the glovebox. Compounds **2** and **3** did not give satisfactory C, H, N analysis because of desolvation. Melting points were recorded in glass capillaries sealed under N_2 and are uncorrected. UV−vis data were recorded on a Hitachi-1200 spectrometer.

$Cr\{Ar'Cr(\mu\text{-}NMe_2)_2\}_2$ (1). About 30 mL of benzene was added to a mixture of $\{Ar'Cr(\mu\text{-}Cl)\}_2$ (0.194 g, 0.20 mmol) and $LiNMe_2$ (0.021 g, 0.40 mmol) at room temperature. The mixture was stirred for 24 h, by which time the solution had become a green/blue color with a brown precipitate. All volatile materials were removed and the green residue was extracted with hexanes (20 mL). The green filtrate was concentrated to *ca.* 3 mL, which yielded X-ray quality green crystals of **1** after storage for several days at 7 °C. Yield: 0.025 g (22.2%). Anal. Calcd. for $C_{68}H_{98}Cr_3N_4$: C, 72.44; H, 8.76; N, 4.97. Found: C, 72.91; H, 8.63; N, 4.59. Mp 227−229 °C (decomposed to a brown oil). UV−vis (hexane, nm [ε, $cm^{-1}\ M^{-1}$]): 656 (1700).

$\{Ar'Mn(\mu\text{-}NMe_2)\}_2\cdot 2C_6H_6$ ($2\cdot 2C_6H_6$). The synthesis, which was analogous to that used for **1**, employed $\{Li(THF)Ar'MnI_2\}_2$ (0.393 g, 0.25 mmol) and $LiNMe_2$ (0.026 g, 0.51 mmol) in benzene (30 mL) and afforded large pink crystals of **2** by storing a hexane/benzene solution of **2** for several days at −18 °C. Yield 0.142 g (57.2%). Mp 224−226 °C. UV−vis (hexane, nm [ε, $cm^{-1}\ M^{-1}$]): 357 (2100), 392 (shoulder).

$\{Ar'Fe(\mu\text{-}NMe_2)\}_2\cdot n\text{-}C_6H_{14}$ ($3\cdot n\text{-}C_6H_{14}$). A similar procedure to that use for **1**, in which $\{Ar'Fe(\mu\text{-}Br)\}_2$ (0.267 g, 0.25 mmol) and $LiNMe_2$ (0.026 g, 0.51 mmol) were employed, afforded X-ray quality colorless crystals of **3** by storing a saturated hexane solution (∼1 mL) of **3** for one week at −18 °C. Yield: 0.156 g (62.7%). Mp: 166−168 °C. UV−vis (hexane, nm [ε, $cm^{-1}\ M^{-1}$]): 446 (350).

$\{Ar^{\#}Co(\mu\text{-}I)(\eta^1\text{-}CH_2{=}NCH_3)\}_2$ (4). The synthesis analogous to that for **1** employed $\{Ar^{\#}Co(\mu\text{-}I)\}_2$ (0.250 g, 0.25 mmol) and $LiNMe_2$ (0.026 g, 0.51 mmol) in hexanes, and afforded X-ray quality blue crystals of **4** after storage for several days at −18 °C. Yield: 0.044 g (16.3%). Anal. Calcd. for $C_{52}H_{60}Co_2I_2N_2$: C, 57.58; H, 5.58; N, 2.58. Found: C, 57.81; H, 5.34; N, 2.26. Mp: 172−174 °C. UV−vis (hexane, nm [ε, $cm^{-1}\ M^{-1}$]): 563 (600), 654 (900), 770 (1300).

X-ray Crystallographic Studies. Suitable crystals of **1**−**4** were selected and covered with a layer of hydrocarbon oil under a rapid flow of argon. They were mounted on a glass fiber attached to a copper pin and placed in the cold N_2 stream on the diffractometer. X-ray data were collected at 90(2) K on a Bruker SMART 1000 diffractometer or on a Bruker SMART Apex II diffractometer with Mo Kα (λ = 0.71073 Å) radiation. Absorption corrections were applied using SADABS.[40] The structures were solved using direct methods and refined by the full-matrix least-squares procedure in SHELXL.[41] All non-hydrogen atoms were refined anisotropically. Hydrogen atoms on the methylene (C25) group in complex **4** were located by a Fourier difference map and other hydrogens in all structures were placed at calculated positions and included in the refinement using a riding model.

Magnetic Studies. The powdered samples of **1**−**4** used for magnetic measurements were sealed under N_2 in 3 mm diameter quartz tubing. The sample magnetization was measured using a Quantum Designs MPMSXL7 superconducting quantum interference magnetometer. For each compound the sample was zero-field cooled to 2 or 5 K and the long moment was measured upon warming to 320 K in an applied field of 0.01 T. To ensure thermal equilibrium between the powdered sample in the quartz tube and the temperature sensor, the long moment at each temperature was measured after 50, 36, 28, 20, and 12 min intervals over the temperature ranges of 2−6, 6−10, 10−25, 25−70, and 70−320 K, respectively; the measurements required *ca.* 20 h for each sample. Diamagnetic corrections of −0.000759, −0.000738, −0.000966, and −0.000639 emu/mol, obtained from tables of Pascal's constants, have been applied to the measured susceptibility of **1**−**4**, respectively.

Results and Discussion

Synthesis and Spectroscopy. The compounds **1**−**4** were synthesized in moderate yields through the reactions of the corresponding aryl metal halide with $LiNMe_2$ in

(27) Edema, J. J. H.; Gambarotta, S.; Spek, A. L. *Inorg. Chem.* **1989**, *28*, 811.
(28) Belforte, A.; Calderazzo, F.; Englert, U.; Strahle, J.; Wurst, K. *J. Chem. Soc., Dalton Trans.* **1991**, 2419.
(29) Chen, H.; Bartlett, R. A.; Dias, H. V. R.; Olmstead, M. M.; Power, P. P. *J. Am. Chem. Soc.* **1989**, *111*, 4338.
(30) Andersen, R. A.; Faegri, K.; Green, J. C.; Haaland, A.; Lappert, M. F.; Leung, W. P.; Rypdal, K. *Inorg. Chem.* **1988**, *27*, 1782.
(31) Bradley, D. C.; Hursthouse, M. B.; Rodesiler, P. F. *J. Chem. Soc., Chem. Commun.* **1969**, 14.
(32) Ellison, J. J.; Power, P. P.; Shoner, S. C. *J. Am. Chem. Soc.* **1989**, *111*, 8044.
(33) Chen, H.; Bartlett, R. A.; Olmstead, M. M.; Power, P. P.; Shoner, S. C. *J. Am. Chem. Soc.* **1990**, *112*, 1048.
(34) Bush, M. A.; Sim, G. A. *J. Chem. Soc., Inorg. Phys. Theor.* **1970**, 611.
(35) Bouwkamp, M. W.; Lobkovsky, E.; Chirik, P. J. *Inorg. Chem.* **2006**, *45*, 2.
(36) Koelle, U.; Fuss, B.; Belting, M.; Raabe, E. *Organometallics* **1986**, *5*, 980.
(37) Clyburne, J. A. C.; McMullen, N. *Coord. Chem. Rev.* **2000**, *210*, 73.
(38) Twamley, B.; Haubrich, S. T.; Power, P. P. *Adv. Organomet. Chem.* **1999**, *44*, 1.
(39) Sutton, A. D.; Ngyuen, T.; Fettinger, J. C.; Olmstead, M. M.; Long, G. J.; Power, P. P. *Inorg. Chem.* **2007**, *46*, 4809.
(40) *SADABS, An Empirical Absorption Correction Program from the SAINTPlus NT*, version 5.0; Bruker AXS: Madison, WI, 1998.
(41) *SHELXL*, version 5.1; Bruker AXS: Madison, WI, 1998.

hexanes or benzene (see reactions 1−4). The different aryl metal halide precursors were selected based on synthetic accessibility, yield and purity. For example, a simple aryl metal halides $\{Ar'Cr(\mu\text{-}Cl)$ and $\{Ar'Fe(\mu\text{-}Br)\}_2$ were used because they could be readily prepared in good yield, whereas a corresponding manganese species was unavailable in pure form. Thus, the easily prepared "ati" salt $\{Li(THF)Ar'MnI_2\}_2$ was used instead. Crystals of **1**−**4** suitable for X-ray crystallography could be readily obtained from hexanes or a mixture of hexanes and benzene.

$$\{Ar'Cr(\mu\text{-}Cl)\}_2 + 2LiNMe_2 \xrightarrow{C_6H_6} \underset{\mathbf{1}}{Cr\{Ar'Cr(\mu\text{-}NMe_2)_2\}_2} \quad (1)$$

$$\{Li(THF)Ar'MnI_2\}_2 + 2LiNMe_2 \xrightarrow{\text{hexanes}} \underset{\mathbf{2}}{\{Ar'Mn(\mu\text{-}NMe_2)\}_2} + 2\,LiI \quad (2)$$

$$\{Ar'Fe(\mu\text{-}Br\}_2 + 2LiNMe_2 \xrightarrow{\text{hexanes}} \underset{\mathbf{3}}{\{Ar'Fe(\mu\text{-}NMe_2)\}_2} + 2\,LiBr \quad (3)$$

$$\{Ar\,Co(\mu\text{-}I)\}_2 + 2LiNMe_2 \xrightarrow{\text{hexanes}} \underset{\mathbf{4}}{\{Ar\,Co(\eta^1\text{-}CH_2{=}NCH_3)(\mu\text{-}I)\}_2} \quad (4)$$

Several attempts were made to synthesize the chromium analogue of **2** or **3** by using various molar ratios of $LiNMe_2$:$\{Ar'Cr(\mu\text{-}Cl)\}_2$. However, only the trimetallic species **1** could be obtained from the reaction mixture. Complexes **2** and **3** were prepared following the same synthetic route as **1**. In these cases, the straightforward dimeric complexes with bridging NMe_2 groups were obtained in good yields. The reaction of $\{Ar'Co(\mu\text{-}Cl)\}_2$ with two equivalents of $LiNMe_2$ was also attempted, but no amido or other characterizable product was found in this case, perhaps due to decomposition of the desired product. As a consequence, the less bulky aryl metal halide $\{Ar^{\#}Co(\mu\text{-}I)\}_2$ was employed; but only **4** could be isolated from the reaction mixture. In contrast to **2** and **3**, the reaction proceeded without elimination of lithium halide and the iodide-bridged species **4** was isolated in low yield.

The reaction sequence by which **4** is produced during the course of the reaction is unknown. However, it is possible that an amide intermediate $\{Ar^{\#}CoNMe_2\}_n$ (n = 1 or 2) is generated initially, which is followed by β-hydrogen elimination of the amido intermediate in accordance with eq 5 to generate a hydride species and a methylimine molecule. The smaller size of the $Ar^{\#}$ ligand and the larger size of the bridging iodides may permit incorporation of the released $H_2C{=}NMe$ molecule into the unreacted $\{Ar^{\#}Co(\mu\text{-}I)\}_2$ to form **4**, while the presumably unstable cobalt hydride decomposes to unidentified products.

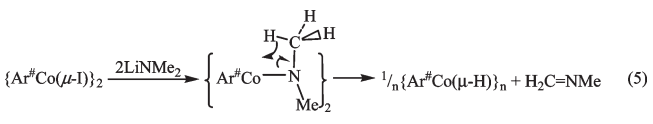

(5)

Complexes **1**−**4** are paramagnetic. The ^1H NMR spectra of **1**, **2**, and **4** show very broad signals, which could not be readily assigned. The UV−visible spectra of **1**−**4** are characterized by intense absorptions below 250 nm, corresponding to the π−π^* transitions within the aryl ligands. In addition, **1** exhibits a very broad moderate-intensity absorption centered at 656 nm (ε = 1700 cm^{-1} M^{-1}). The presence of two different chromium centers with either C_s or D_{2h} local symmetry presumably yields different unresolved splittings of the ^5D ground state. Complex **2** features a strong-intensity absorption centered at 357 nm (ε = 2100 cm^{-1} M^{-1}) and has a featureless spectrum in the visible region as is expected for manganese(II) ion with a high-spin $3d^5$ electronic configuration and a ^6S ground state. The crystals of **3** are almost colorless, and they have a low-intensity absorption centered at 446 nm (ε = 350 cm^{-1} M^{-1}) with an otherwise featureless visible spectrum. Complex **4** exhibits three absorption bands at 563 (ε = 600 cm^{-1} M^{-1}), 654 (ε = 900 cm^{-1} M^{-1}), and 770 nm (ε = 1300 cm^{-1} M^{-1}), consistent with a cobalt(II) ion in a distorted tetrahedral coordination environment with a ^4F ground state.

Structures. The structures of **1**−**4** were determined by X-ray crystallography. Important data collection and refinement parameters for **1**−**4** are presented in Table 1, and selected structural data are given in Tables 2−4. The structures of **1**−**4** are shown in Figures 1−4, respectively.

The chromium complex **1** exhibits an unusual trinuclear structure with a linear metal array. Structures featuring linear arrays of three or more Cr(II) centers are rare and have only been obtained by using multidentate ligand platforms.[42,43] Molecules of **1** have crystallographically imposed inversion centers at the central chromium(II) ion, which has a planar coordination geometry and is bound to four bridging NMe_2 ligands with N(1)−Cr(2)−N(2) and N(1)−Cr(2)−N(2A) angles of 97.38(7)° and 82.62(7)°, respectively. The Cr(2)−N(1) and Cr(2)−N(2) bond lengths, 2.113(2) and 2.107(2) Å, are similar to those found in the chromate ion pair salt $[Cr(NHC_6H_3\text{-}2,6\text{-}{}^iPr_2)_4][Li(THF)_2]$ (2.09(2) to 2.133(2) Å).[44] The two outer chromium(II) ions (Cr(1) and Cr(1A)) are coordinated to two bridging NMe_2 ligands and a terminal aryl ligand. The interligand angles at Cr(1) are 163.55(8)°, 110.11(7)°, and 86.21(8)°, consistent with a distorted T-shaped geometry. Such coordination geometry is thus highly unusual for chromium and may be contrasted with the *quasi*-square planar arrangement in $\{Ar'Cr(\mu\text{-}Cl)\}_2$[39] and $\{3,5\text{-}{}^iPr_2Ar^*Cr(\mu\text{-}Me)\}_2$ (3,5-$^iPr_2$-Ar* = C_6H-2,6-(C_6H_2-2,4,6-$^iPr_3$)$_2$-3,5-$^iPr_2$),[45] where the chromium(II) atoms interact strongly with the ipso carbon from one of the flanking aryl rings. The distorted T-shaped geometry appears to be precedented only by that in the alkoxide $\{Cr(OCBu^t{}_3)_2(\mu\text{-}Cl)Li(THF)_2\}$[46] and is generally not found in chromium(II) amides, where the distorted trigonal planar geometry in complexes such as

(42) Cotton, F. A.; Daniels, L. M.; Murillo, C. A.; Pascual, I. *J. Am. Chem. Soc.* **1997**, *119*, 10223.
(43) Ismayilov, R. H.; Wang, W. Z.; Lee, G. H.; Chien, C. H.; Jiang, C. H.; Chiu, C. L.; Yeh, C. Y.; Peng, S. M. *Eur. J. Inorg. Chem.* **2009**, 2110.
(44) Danopoulos, A. A.; Hankin, D. M.; Wilkinson, G.; Cafferkey, S. M.; Sweet, T. K. N.; Hursthouse, M. B. *Polyhedron* **1997**, *16*, 3879.
(45) Ni, C. B.; Power, P. P., *Organometallics* [Online early access] DOI: 10.1021/om900724p. Published Online Oct 29, 2009..
(46) Hvoslef, J.; Hope, H.; Murray, B. D.; Power, P. P. *J. Chem. Soc., Chem. Commun.* **1983**, 1438.

Table 1. Selected Crystallographic Results for **1**−**4**

	1	**2**·2C_6H_6	**3**·*n*-hexane	**4**
formula	$C_{68}H_{98}Cr_3N_4$	$C_{76}H_{98}Mn_2N_2$	$C_{70}H_{100}Fe_2N_2$	$C_{52}H_{60}Co_2I_2N_2$
fw, g/mol	1127.54	1149.44	1081.27	1084.68
color, habit	green, block	pink, rod	colorless, plate	blue, plate
cryst system	*Pbca*	$P2_1/n$	$P2_1/n$	$P\bar{1}$
a, Å	17.2249(11)	16.9367(7)	16.5044(15)	8.2491(10)
b, Å	16.8147(11)	10.5787(5)	10.4869(9)	11.5970(14)
c, Å	21.8935(14)	18.7807(8)	18.9310(17)	13.2764(16)
α, deg	90	90	90	72.0510(10)
β, deg	90	104.1120(10)	103.3290(10)	83.389(2)
γ, deg	90	90.00	90	78.197(2)
V, Å^3	6341.0(7)	3263.4(2)	3188.3(5)	1180.9(2)
Z	4	2	2	1
d_{calcd}, Mg/m^3	1.191	1.170	1.126	1.525
θ range, deg	1.86−27.50	2.95−31.51	2.69−25.20	2.81−27.56
μ, mm^{-1}	0.605	0.430	0.495	2.045
obs data, $I > 2\sigma(I)$	5259	6682	4629	4867
R1 (obs data)	0.0400	0.0301	0.0393	0.0227
wR2 (all data)	0.1183	0.0832	0.1095	0.0588

Table 2. Selected Distances (Å) and Angles (deg) for **1**

Cr1···Cr2	2.9515(3)	C1−Cr1−Cr2	147.61(6)
Cr1−C1	2.123(2)	Cr1−Cr2−Cr1A	180.0
Cr1−N1	2.072(2)	C1−Cr1−N1	163.55(8)
Cr1−N2	2.0047(18)	C1−Cr1−N2	110.11(7)
Cr2−N1	2.113(2)	N1−Cr1−N2	86.21(8)
Cr2−N2	2.1072(17)	Cr1−N1−Cr2	89.70(9)
N1−C31	1.453(3)	Cr1−N2−Cr2	91.71(7)
N1−C32	1.467(3)	N1−Cr2−N2	97.38(7)
		N1−Cr2−N2A	82.62(7)

Table 3. Selected Distances (Å) and Angles (deg) for **2** and **3**

	2	**3**
M1···M1A	2.9479(3)	2.7241(6)
M1−C1	2.1076(8)	2.056(2)
M1−N1	2.0938(8)	2.0206(18)
M1−N1A	2.1247(9)	2.0354(19)
N1−C31	1.4608(14)	1.476(3)
N1−C32	1.4779(13)	1.465(3)
C1−M1−N1	144.14(3)	138.51(8)
C1−M1−N1A	122.99(3)	124.99(8)
N1−M1−N1A	91.34(3)	95.62(7)
M1−N1−M1A	88.66(3)	84.38(7)
C1−M1−M1A	165.49(3)	169.76(6)

Table 4. Selected Distances (Å) and Angles (deg) for **4**

Co1···Co1A	3.628(3)	C1−Co1−N1	117.69(8)
Co1−C1	2.012(2)	C1−Co1−I1A	112.25(6)
Co1−N1	2.0472(19)	C1−Co1−I1	126.49(6)
Co1−I1	2.6898(4)	I1−Co1−I1A	95.035(13)
Co1−I1A	2.6825(4)	C25−N1−C26	118.0(2)
N1−C25	1.262(3)	C25−N1−Co1	122.99(19)
N1−C26	1.451(3)	C26−N1−Co1	118.95(17)
		Co1−I1−Co1A	84.965(13)

{Cr(NRR′)(*μ*-NRR′)}$_2$ (R = 3,5-Me$_2$-C$_6$H$_3$, R′ = adamantyl)[47] and {Cr(N^{i}Pr$_2$)(*μ*-N^{i}Pr$_2$)}$_2$[27] is normal. In **1**, the Cr−C distance (2.123(2) Å) is slightly longer than those in Mes$_2$Cr(THF)$_2$ (2.083(11) Å),[48] Mes$_2$Cr(bipy)$_2$ (2.098(14) Å),[48] and {Ar′Cr(*μ*-Cl)}$_2$ (2.041(3) Å).[39] The Cr(1)−N bonds of 2.072(2) and 2.005(2) Å are slightly shorter than those of the central chromium(II) ion, perhaps because of the lower coordination numbers of Cr(1) and Cr(1A). The

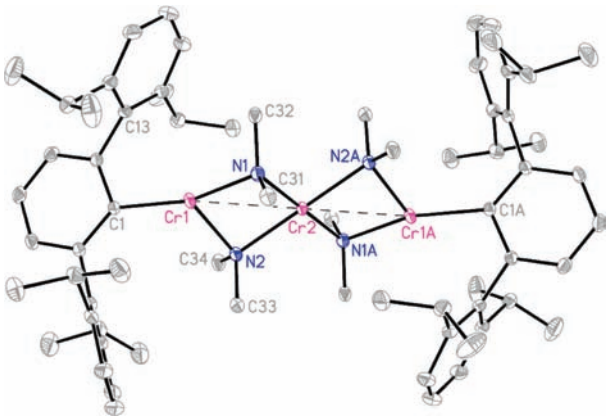

Figure 1. Thermal ellipsoid plot (30%) of **1** without H atoms.

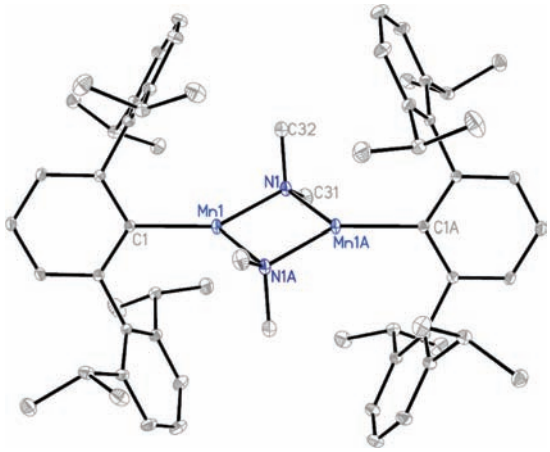

Figure 2. Thermal ellipsoid plot (30%) of **2** without H atoms.

Cr$_2$(*μ*-N)$_2$ cores in **1** are folded along the Cr− −Cr axis with a fold angle of ∼34.11(4)°, which is similar, but larger than that of 24.0(3)° observed in {Cr(NRR′)(*μ*-NRR′)}$_2$.[47] The Cr− −Cr separation in **1** is 2.9515(3) Å, which lies between the value of 2.838(2) Å observed in {Cr(NCy$_2$)(*μ*-NCy$_2$)}$_2$[42] (Cy = cyclohexyl) and the value of 3.150(1) Å found in{Cr(*μ*-NPh$_2$)(NPh$_2$)(THF)}$_2$,[49] but is

(47) Ruppa, K. B. P.; Feghali, K.; Kovacs, I.; Aparna, K.; Gambarotta, S.; Yap, G. P. A.; Bensimon, C. *J. Chem. Soc., Dalton Trans.* **1998**, 1595.

(48) Edema, J. J. H.; Gambarotta, S.; Vanbolhuis, F.; Smeets, W. J. J.; Spek, A. L.; Chiang, M. Y. *J. Organomet. Chem.* **1990**, *389*, 47.

(49) Edema, J. J. H.; Gambarotta, S.; Meetsma, A.; Spek, A. L.; Smeets, W. J. J.; Chiang, M. Y. *J. Chem. Soc., Dalton Trans.* **1993**, 789.

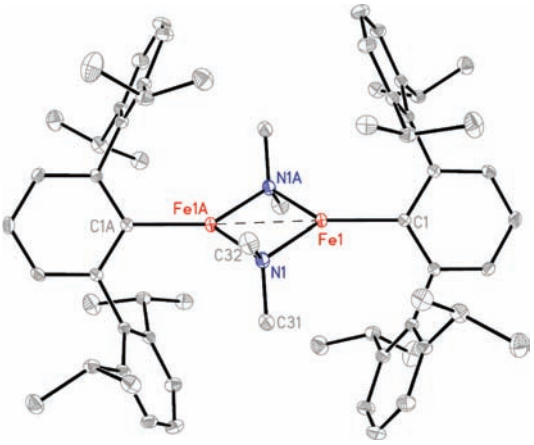

Figure 3. Thermal ellipsoid plot (30%) of **3** without H atoms.

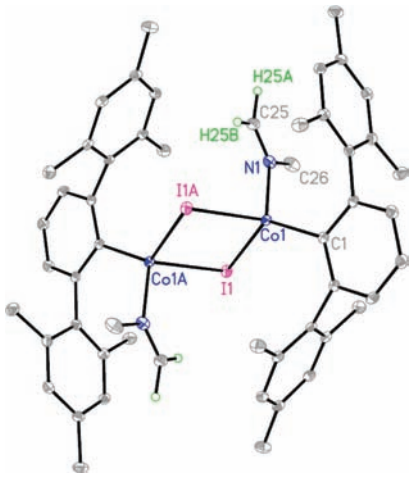

Figure 4. Thermal ellipsoid plot (30%) of **4**. The hydrogen atoms, except for H25A and H25B, are not shown.

significantly longer than that of 2.67(1) Å in *trans*-{(η^5-C_5H_5)Cr(NO)(μ-NMe_2)}$_2$.[34] This might be the result of the steric effect of the bulky terphenyl ligand on the terminal metal centers.

Crystals of **2** and **3** are isomorphous and the structures of the two complexes are very similar. They are characterized by a crystallographically required inversion center midway between the metal ions. Dimerization occurs through the almost symmetric bridging of the metal ions by two $-NMe_2$ ligands. The Ar′ group is terminally bound to each metal to yield a distorted, almost planar, trigonal coordination geometry. For **2**, the Mn−C bond length, 2.1076(8) Å, is similar to those in the two-coordinate diaryl species $MnMes^*_2$ (Mes* = C_6H_2-2,4,6-^{t}Bu$_3$, 2.108(2) Å),[50] $MnAr^{\#}_2$ (2.095(3) Å),[51] and the three-coordinate complex {HC(CMeNAr)$_2$}MnPh (Ar = 2, 6-^{i}Pr$_2$-C_6H_3, 2.077(6) Å).[52] The Mn−N distances (2.0938(8) and 2.1247(9) Å) are similar, but are somewhat shorter than those bridging Mn−N distances in {Mn(N^{i}Pr$_2$)(μ-N^{i}Pr$_2$)}$_2$ (2.139(5) Å)[28] and {Mn[N(SiMe$_3$)$_2$]-[μ-N(SiMe$_3$)$_2$]}$_2$ (2.174(3) Å),[53] possibly because of the smaller steric requirement of $-NMe_2$. Although the $Mn_2(\mu$-N$)_2$ core is symmetric and almost perfectly square, the external N-Mn-C angles differ by over 21°. This difference is also probably steric in origin as a result of transannular terphenyl-terphenyl interactions. The Mn−−−Mn separation is 2.9479(3) Å, which lies between that of 2.811(1) Å in {Mn[N(SiMe$_3$)$_2$][μ-N(SiMe$_3$)$_2$]}$_2$[53] and that of 3.024(2) Å in Mn{Mn[N(SiMe$_3$)$_2$](μ-NH-C_6H_3-2,6-^{i}Pr$_2$)$_2$}$_2$.[54]

The structure of **3** is very similar to that of **2**. The main difference is that the bond lengths to the iron(II) ion are 0.05−0.09 Å shorter than those to the manganese(II) ion, a difference which is consistent with the smaller iron(II) ionic radius.[55] The Fe-C bond length (2.056(2) Å) is very similar to those in the two-coordinate complexes $FeMes^*_2$ (2.058(6) Å),[50,56] $FeAr^{\#}_2$ (2.040(3) Å),[51] and Ar′FeN(H)Ar$^{\#}$ (2.046(2) Å).[57] The Fe-N distances (2.0206(18) and 2.0354(19) Å) are almost equal and are similar to the bridging distances in {Fe(NPh$_2$)(μ-NPh$_2$)}$_2$ (2.036(3) Å).[58] They are longer than those in M[($^{i\mathrm{Pr}}$PDEA)Fe(μ-NMe$_2$)] ($^{i\mathrm{Pr}}$PDEA = (2,6-^{i}Pr$_2$-C_6H_3N=CMe$_2$)$_2$$C_5H_3$N, M = Li or K, 1.9773(16) Å)[35] and {Fe(CO)$_3$(μ-NH$_2$)}$_2$ (1.98(2) Å),[59] but shorter than the average bridging distance of 2.085 Å in the crowded complex {Fe[N(SiMe$_3$)$_2$][μ-N(SiMe$_3$)$_2$]}$_2$.[58] The distortion in the C−Fe−N angles (C(1)−Fe(1)−N(1) = 138.53(8)°; C(1)−Fe(1)−N(1A) = 124.99(8)°) is not as large as that in **2**, but the Fe---Fe separation of 2.7241(6) Å is very similar to the 2.715(1) Å and 2.663(1) Å separations observed in {Fe(NR$_2$)(μ-NR$_2$)}$_2$ (R = Ph or SiMe$_3$).[58]

The structure of **4**, which bears a resemblance to that of the dimer {Ar$^{\#}$Co(μ-Br)(THF)}$_2$,[60] is dimerized through two bridging iodides and is characterized by an inversion center midway between the cobalt(II) ions as in **2** and **3**. Thus, the $Co_2(\mu$-I$)_2$ unit is planar with I−Co−I and Co−I−Co angles of 95.035(13)° and 84.965(13)°, respectively. Each cobalt is also bound to a terminal Ar$^{\#}$ ligand and a CH_2=NCH_3 ligand, which was probably formed via hydrogen elimination from the NMe_2 group. The dehydrogenation of an NMe_2 ligand was also observed in the formation of (PMe$_2$Ph)Cl$_2$W(μ-NMe$_2$)(μ-η^1,η^2-CHCH$_2$)(μ-η^2,η^1-CH$_2$NMe)WCl(NMe$_2$)(PMe$_2$Ph);[61,62] however, unlike the μ and η^2 coordination mode in that tungsten complex, the CH$_2$=NMe ligand in **4** adopts a σ only coordination through the lone pair on nitrogen. This may be due to the tendency of cobalt(II) complexes to prefer tetrahedral coordination. The Co-C bond length (2.012(2) Å) is similar to those observed in $CoAr^{\#}_2$ (2.001(3) Å),[51] {Li(OEt$_2$)Ar′CoI$_2$}$_2$ (2.004(5) and

(50) Wehmschulte, R. J.; Power, P. P. *Organometallics* **1995**, *14*, 3264.
(51) Kays, D. L.; Cowley, A. R. *Chem. Commun.* **2007**, 1053.
(52) Chai, J. F.; Zhu, H. P.; Fan, H. J.; Roesky, H. W.; Magull, J. *Organometallics* **2004**, *23*, 1177.
(53) Murray, B. D.; Power, P. P. *Inorg. Chem.* **1984**, *23*, 4584.
(54) Kennepohl, D. K.; Brooker, S.; Sheldrick, G. M.; Roesky, H. W. *Z. Natuaforsch. B: Chem. Sci.* **1992**, *47*, 9.
(55) Emsley, J. *The Elements*; Oxford University Press: Oxford, U.K., 1998.
(56) Muller, H.; Seidel, W.; Gorls, H. *Angew. Chem., Int. Ed.* **1995**, *34*, 325.
(57) Ni, C. B.; Fettinger, J. C.; Long, G. J.; Power, P. P. *Inorg. Chem.* **2009**, *48*, 2443.
(58) Olmstead, M. M.; Power, P. P.; Shoner, S. C. *Inorg. Chem.* **1991**, *30*, 2547.
(59) Dahl, L. F.; Costello, W. R.; King, R. B. *J. Am. Chem. Soc.* **1968**, *90*, 5422.
(60) Ellison, J. J.; Power, P. P. *J. Organomet. Chem.* **1996**, *526*, 263.
(61) Ahmed, K. J.; Chisholm, M. H.; Folting, K.; Huffman, J. C. *J. Chem. Soc., Chem. Commun.* **1985**, 152.
(62) Ahmed, K. J.; Chisholm, M. H.; Folting, K.; Huffman, J. C. *J. Am. Chem. Soc.* **1986**, *108*, 989.

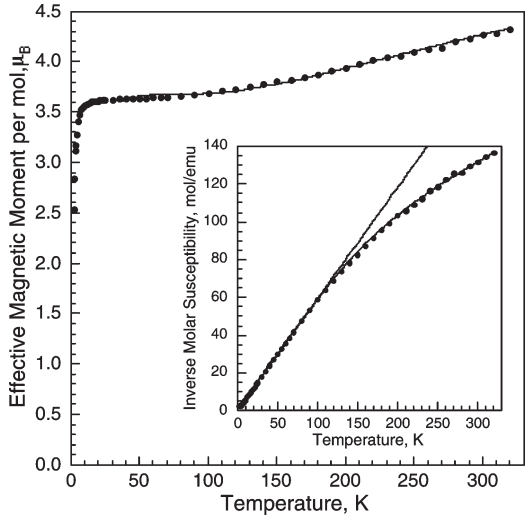

Figure 5. Temperature dependence of μ_{eff} per mol of **1**. Inset: The temperature dependence of $1/\chi_M$ of **1** and a linear Curie−Weiss law fit between 2 and 100 K. In both plots, the solid line through the data points corresponds to a 25−320 K fit with $g = 2$, $S = 2$, $J = -47$ cm^{-1}, and $J_{13} = -25(1)$ cm^{-1}.

1.998(5) Å),[39] and {Ar#Co(μ-Br)(THF)}$_2$ (2.053(8) Å).[60] The Co−I distances (2.6898(4) and 2.6825(4) Å) are essentially the same, and are comparable to those in {Ph$_3$POCoI(μ-I)}$_2$ (2.647 and 2.652 Å).[63] The Co···Co separation is 3.628(3) Å, which is consistent with the absence of bonding interaction between two cobalt(II) ions discussed below. The Co−N distance, 2.0472(19) Å, is within the range of bond distances for numerous cobalt(II) imine complexes. The N(1)-C(25) distance is 1.262(3) Å, which is consistent with the double bond character between the N(1) and C(25) atoms, and is, as expected, considerably shorter than the N(1)−C(26) distance (1.451(3) Å).

Magnetic Properties. The magnetic properties of **1** (Figure 5) indicate that it is essentially a magnetically dilute complex with intramolecular antiferromagnetic exchange interactions between the three chromium(II) ions. Below 100 K the inverse molar magnetic susceptibility ($1/\chi_M$) is linear (the inset to Figure 5) and yields a Weiss temperature θ of −1.0 K, a Curie constant, C, of 1.702 emu K/mol, and a corresponding effective magnetic moment (μ_{eff}) of 3.69 μ_B per mole. Because of the intramolecular exchange interactions present in **1**, this value is significantly below the spin-only μ_{eff} of 4.90 μ_B expected for a single isolated chromium(II) ion or the corresponding 8.49 μ_B expected for three isolated chromium(II) ions. Also, because of the magnetic exchange, the μ_{eff} value of **1** decreases almost linearly from 4.32 μ_B at 320 K to 3.75 μ_B at 130 K, remains approximately constant at *ca.* 3.7 μ_B between 80 and 20 K and then below 20 K decreases to 2.53 μ_B at 2 K. The decrease in μ_{eff} below 20 K is probably due to zero field splitting of the magnetic ground state of either two or all three of the chromium(II) ions. Because of the presence of the structurally different chromium(II) ions, no attempt had been made herein to model their combined zero-field splittings.

(63) Gorter, S.; Hinrichs, W.; Reedijk, J.; Rimbault, J.; Pierrard, J. C.; Hugel, R. P. *Inorg. Chim. Acta* **1985**, *105*, 181.

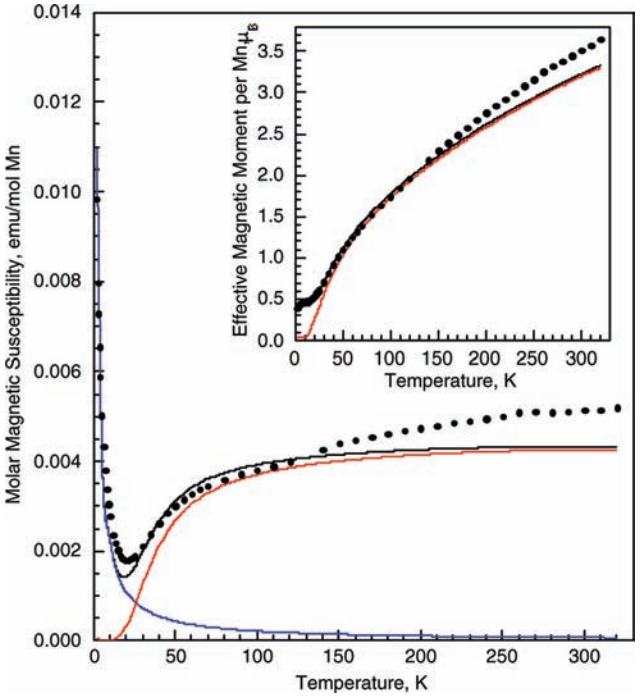

Figure 6. Temperature dependence of χ_M of **2**. Inset: The temperature dependence of the μ_{eff} of **2**. In these plots, the solid red line corresponds to a fit between 2 and 120 K for magnetic exchange between the two manganese(II) ions with $g = 2$, $S = 5/2$, and $J = -38(1)$ cm^{-1}. The blue line corresponds to 0.5(1) wt% of a paramagnetic manganese(II) impurity with $g = 2$, $S = 5/2$, and $J = 0$ cm^{-1}. The black lines correspond to the sum of the red and blue components.

As might be expected on the basis of their structural similarity, the magnetic properties of compounds **2** and **3** are rather similar as is shown in Figures 6 and 7; because the two exchange-coupled metal ions in these compounds are crystallographically equivalent, the results in the figures are presented per metal ion. In both compounds, $1/\chi_M$ is nonlinear because of the presence of antiferromagnetic interactions between the two metal ions. Further, at very low temperatures χ_M increases to a maximum at 2 K. This behavior is typical of antiferromagnetically coupled dimers in the presence of a trace amount of high-spin monomeric paramagnetic impurities. Thus the χ_M values of **2** and **3** observed between 2 and 120 K have been fit with the $\mathscr{H} = -2J(\mathbf{S}_1 \cdot \mathbf{S}_2)$ Hamiltonian for exchange coupled dimers[64,65] with a trace impurity component with $J = 0$, corresponding to a monomeric impurity. In the case of the iron(II) dimer **3**, a temperature-independent paramagnetic susceptibility ($N\alpha$) has been included in the fit. The results of these fits are shown as the solid lines in Figures 6 and 7. The temperature dependence of χ_M observed for **2** and **3** between 2 and 320 K are not well fit with a single J value, indicating that J is probably not independent of temperature, most likely as a result of small changes in the bridging geometry upon cooling. Indeed, for both compounds there is a small inflection in the observed χ_M near 150 K. As a consequence, χ_M has been fit between 2 and

(64) Details of the Hamiltonian used for these fits are given in the Supporting Information provided with reference 65.

(65) Wolf, R.; Ni, C.; Nguyen, T.; Brynda, M.; Long, G. J.; Sutton, A. D.; Fischer, R. C.; Fettinger, J. C.; Hellman, M.; Pu, L. H.; Power, P. P. *Inorg. Chem.* **2007**, *46*, 11277.

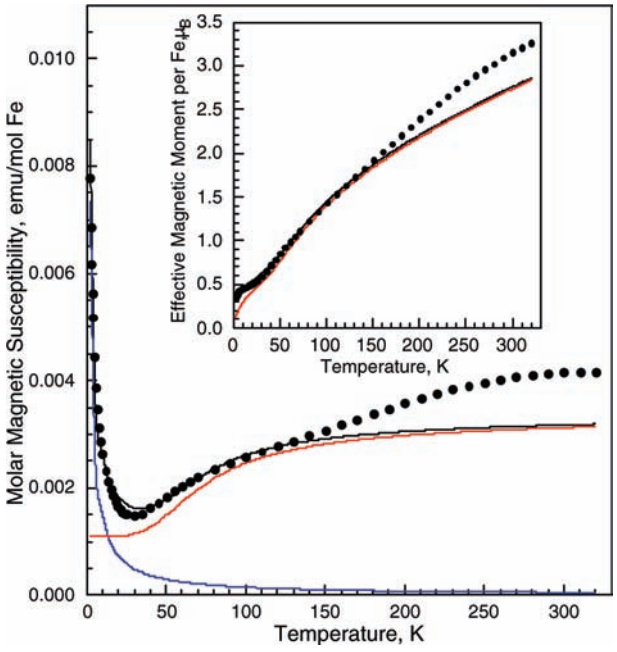

Figure 7. Temperature dependence of χ_M of **3**. Inset: The temperature dependence of the μ_{eff} of **3**. In these plots the solid red line corresponds to a fit between 2 and 120 K for magnetic exchange between the two high-spin iron(II) ions with $g = 2$, $S = 2$, $J = -75(3)$ cm^{-1}, and $N\alpha = 0.00110(8)$ emu/mol Fe. The blue line corresponds to 0.5(1) wt % of a paramagnetic high-spin iron(II) impurity with $g = 2$, $S = 2$, and $J = 0$ cm^{-1}. The black lines correspond to the sum of the red and blue components.

120 K; fits between 2 and 320 K lead to slightly more negative J values than those reported below.

The reasons for the differences in the antiferromagnetic exchange constant observed for compounds **2** and **3** are discussed in the Supporting Information on the basis of the details of the bonding at the metal ions. Further, to better understand the reason for the somewhat unexpected temperature dependence of the antiferromagnetic exchange constant J, observed in **2** and **3**, numerical methods have been used to determine the J value that is most consistent with each of the χ_M values observed between 120 and 320 K, see the Supporting Information and Figure S1 for more details. In the absence of any knowledge of changes in the structures of **2** and **3** with temperature, proposed changes in J must remain tentative both because the changes are rather larger than might be expected and are larger than any previously reported[66] changes in J with temperature.

The magnetic properties of **4** are rather unexpected and unusual as is revealed by the large, almost constant χ_M of ~0.016 emu/mol Co observed between ~150 and 320 K, see Figure S2 in the Supporting Information. This large constant value of χ_M is unexpected for a presumably dilute paramagnetic insulating compound and these results are presented in the Supporting Information because we have been unable to detect any discrepancy in the observed results.

Conclusions

A series of dimethylamido (NMe_2) derivatives of chromium(II), manganese(II), and iron(II), as well as a $CH_2{=}NCH_3$ coordinated Co(II) complex, which is derived from decomposition of an amide, have been prepared by reactions of the aryl metal halides with $LiNMe_2$. The species are rare examples of the well-characterized divalent later first-row transition metal complexes of the parent diorganoamido ligand NMe_2. The reaction chemistry of these complexes is under investigation.

Acknowledgment. We thank the National Science Foundation (CHE-0641020) for financial support, Dr. James C. Fettinger for crystallographic assistance, and Peter Klavins for assistance in magnetization measurements.

Supporting Information Available: Crystallographic information files (CIFs) for **1**−**4** and detailed discussions of magnetic studies. These materials are available free of charge via the Internet at http://pubs.acs.org.

(66) Güdel, H. U.; Furrer, A. *Mol. Phys.* **1977**, *33*, 1335.